Scanning Tunneling Microscopy Observations of Benzene Molecules on the Rh(111)-(3×3)(C_6H_6+2CO) Surface

H. Ohtani,[a] R. J. Wilson, S. Chiang, and C. M. Mate
IBM Research Division, Almaden Research Center, San Jose, California 95120
(Received 22 February 1988)

Scanning tunneling microscopy (STM) images of the (3×3) superlattice of benzene and carbon monoxide coadsorbed on the Rh(111) surface reveal a well-ordered array of ringlike features associated with individual benzene molecules, while CO is not resolved. Images further show translational domain boundaries, step-edge structures, and evidence for surface diffusion. The origin of the STM image contrast of these molecules and implications for STM imaging of other molecular adsorbates are briefly discussed.

PACS numbers: 68.35.Bs, 61.16.Di

Scanning tunneling microscopy (STM) has been proven to be a very powerful tool for atomic resolution imaging of surfaces. This technique has been successfully applied to semiconductor and metal surfaces, both with and without atomic adsorbates.[1] Early results for molecular adsorbates on metal surfaces have been somewhat less encouraging. For example, chemisorbed carbon monoxide molecules have not been resolved on Pt(100) surfaces, even though the CO-induced restructuring of the metal surface was observed.[2] Images of Cu phthalocyanine on Ag surfaces[3] showed low symmetry and resolution, which was interpreted in terms of molecular motion induced by the electric field gradients near the tip. The difficulties in imaging of molecular adsorbates have been thought to be due either to rapid surface diffusion, possibly augmented by electric fields, or to the absence of molecular orbitals near the Fermi level (E_F), which are accessible by STM.

In this Letter, we report the first real-space images of an ordered array of coadsorbed molecules on a clean metal surface. This allows us to study, for the first time, the source of STM image contrast for different molecules under the same experimental conditions. The system studied is the ordered (3×3) superlattice of coadsorbed benzene (C_6H_6) and CO on a Rh(111) surface, which has been well characterized by other surface techniques.[4-6] The detailed geometry of this 3×3 overlayer, as determined with a dynamical LEED analysis,[6] is shown in Fig. 1. The unit cell contains one flat-lying benzene molecule and two upright CO molecules, all chemisorbed over hcp-type threefold hollow sites which, as opposed to fcc-type hollow sites, are directly above second-layer Rh atoms. STM images of this structure reveal individual benzene molecules as threefold ringlike features. Carbon monoxide is not resolved within this structure, as in previous STM work.[2] We analyze the structure of the overlayer at step edges and domain boundaries and find evidence for diffusion of benzene molecules. Our observations are an important step towards real-space imaging of surface-molecule interactions.

The sample was prepared and analyzed in a surface preparation and analysis chamber connected to the STM chamber by internal transfer mechanisms, which is described elsewhere.[7] The Rh(111) sample was cleaned by repeated cycles of 1-keV ion bombardment and heating at 1000°C in the presence of 4×10^{-5} Torr Ar and 8×10^{-10} Torr O_2. The sample was then annealed at 800°C for 10 min. Azimuthal orientation of the crystal was determined by comparison of LEED spot intensities for the clean Rh(111) sample with data in the literature.[8] The Rh(111)-(3×3)(C_6H_6+2CO) structure was obtained by dosing, at room temperature, with 2×10^{-7} Torr s of CO followed by saturation of the surface with 3.6×10^{-6} Torr s of benzene. A sharp (3×3) LEED pattern was verified before and after the STM experiments. The clean Rh(111) surface has not been examined because it becomes contaminated with CO in times comparable to those required for instrumental drifts to

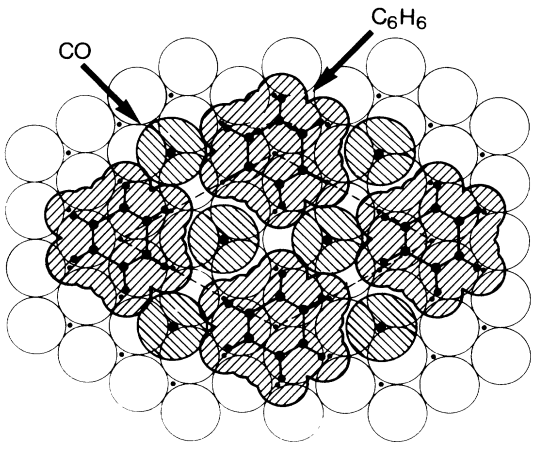

FIG. 1. The structure for Rh(111)-(3×3)(C_6H_6+2CO) determined by LEED crystallography (Ref. 6). Large circles and small dots represent the first- and second-layer metal atoms, respectively.

reach acceptable levels. STM images were obtained in the constant-current slow-scan mode (0.5 Hz/line)[1] for tip biases varying from -2 V to 2 V. Higher biases were useful primarily for tip sharpening. Images obtained by tunneling into empty states of the sample showed more corrugation than filled-state images and are presented exclusively here. A fuller account of this work will be given later.[9]

The STM image, shown in Fig. 2(a), reveals a gentle 0.4-Å corrugation with a (3×3) periodicity (8.1 Å×8.1 Å) extending over an ordered step with a (100) face. The protrusions in these images can be compared with the LEED model of Fig. 1, which suggests that each bump represents a benzene molecule. Using the known scan distances and the LEED assignment for the benzene binding site, we map each terrace onto a mesh representing the top two layers of Rh atoms in a fcc lattice, as shown in Fig. 2(b). A constant height has been subtracted from the upper (left) terrace to improve the image contrast by reducing the step (S) discontinuity. The assumption that the benzene binding site is the same on both terraces allows the unambiguous determination of the azimuthal orientation of the crystal by STM alone, which agrees with the LEED assignment.

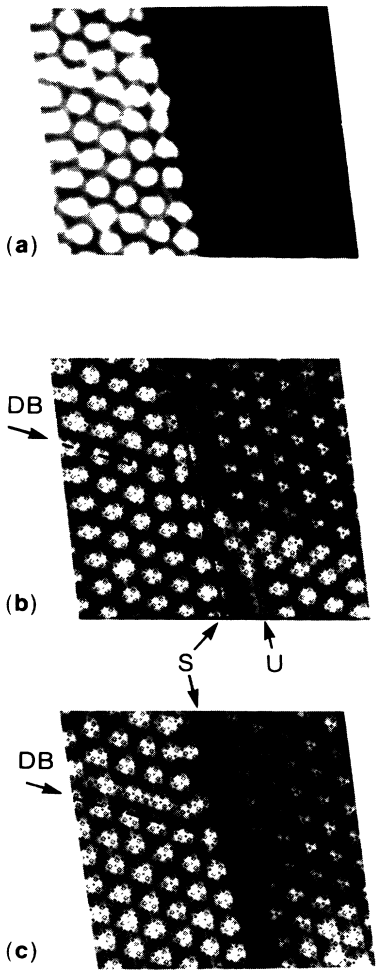

FIG. 2. Three images of the 3×3 superlattice extending across an atomic step. For each terrace, the first- and second-layer Rh atoms are represented by big and small lozenges, respectively. Images were recorded with tip bias $V_t = -1.25$ V and tunnel current $i_t = 4$ nA. (a),(b) Images derived from the same data, (c) image recorded about 10 min later.

Upon close examination, several interesting features in Fig. 2 become apparent. First, benzene evidently prefers to bind at sites adjacent to metal atoms which form the step edge. Second, a translational domain boundary (DB), observable on the upper terrace, preserves the hcp hollow binding site. Third, by comparison of Fig. 2(b) and 2(c), which were recorded about 10 min apart, it can be seen that two benzene molecules, to the lower right of the near vertical domain boundary, have shifted in the latter image into (3×3) lattice positions. Also, an unknown disturbance (U), which may be associated with diffusion of CO or benzene along a row in the lower terrace in Fig. 2(b), has disappeared in Fig. 2(c), whereas the row of molecules just above the domain boundary on the upper terrace take on this disturbed character in Fig. 2(c). These disturbances probably represent a time-averaged image of molecules moving between sites.

Higher-resolution images of the internal structure of the 3×3 cells were obtained by our maximizing the corrugation by adjustment of the tip bias voltage (V_t), tunnel current (i_t), and tip structures. At a given bias voltage, we found that increasing the tunnel current led to an increase in the corrugation and to the appearance of a dip at the center of the protrusions. When the voltages were as large as those used for Fig. 3(a), obtained with $V_t = -1.4$ V and $i_t = 8$ nA, we could not raise the current sufficiently to observe this dip because other instabilities became apparent, as shown. Flat-topped, 2-Å-high, nearly cylindrical structures were observed. The simplest explanation for the instabilities in this image involves the hopping of benzene molecules between equivalent sites, formation of benzene vacancies (V), and modifications to the tip (T). These instabilities are smaller than, but similar to, those reported for Cu phthalocyanine.[3] Figure 3(b) shows a 2-Å-high, ringlike structure, which we observed for $V_t = -0.01$ V and $i_t = 2$ nA. Similar features were observed at $V_t = -0.5$ V with 0.5-Å corrugation. The use of low bias voltages, as in previous work on Au(111),[10] appears to be advantageous for our obtaining small tunnel gaps, which provide larger corrugations, while maintaining reasonable tunnel currents.

Figure 4(a) shows a perspective view of the (3×3) structure which emphasizes the ringlike character and expands the dynamic range of the images. The typical threefold character and the lateral dimensions of the protrusions corroborate the LEED assignment of these pro-

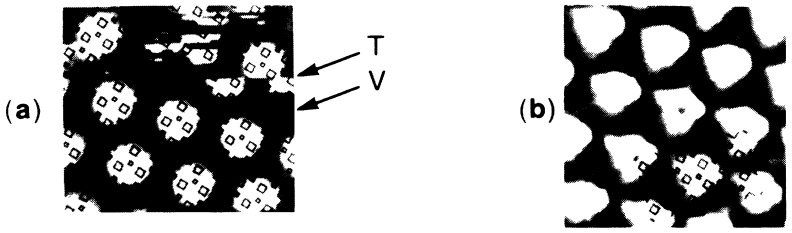

FIG. 3. (a) At high bias the benzene images become flat topped, nearly cylindrical, and 2 Å high, but the tip and surface appear unstable. (b) At lower bias, $|V_t| < 0.5$ V, a nominally threefold structure with a depression at the center is observed. According to the superimposed mesh based on the LEED model, the lobes appear to be localized between, rather than over, the underlying metal atoms.

trusions to benzene molecules adsorbed at hollow sites but is not sufficient to determine the mesh registration uniquely. Rapid diffusion of CO molecules might be a problem on some surfaces, but in this system, one would expect the CO molecules to be locked into the ordered 3×3 lattice formed by stationary benzene molecules. In Fig. 4(a), some protrusions, about 0.2 Å high, are seen close to the positions expected for CO, but these features are so small that they may represent minor tip distortions. Improvements in lateral resolution will be necessary to measure the 1.5-Å C–C bonds of benzene and observe proposed Kekulé distortions of the benzene ring.[6]

At the other extreme, we show a wide-scan image in Fig. 4(b) which displays a variety of steps and defects. The sharp, monatomic step in the middle of the image lies along a $(\bar{1}01)$ direction so that the step has the relatively open face of a (100)-type square lattice, as does the double step in this image. The rougher step shown at the left of the image has a (111)-type close-packed face. The observation of molecules near these steps opens the door for further studies of chemistry and diffusion on stepped surfaces.

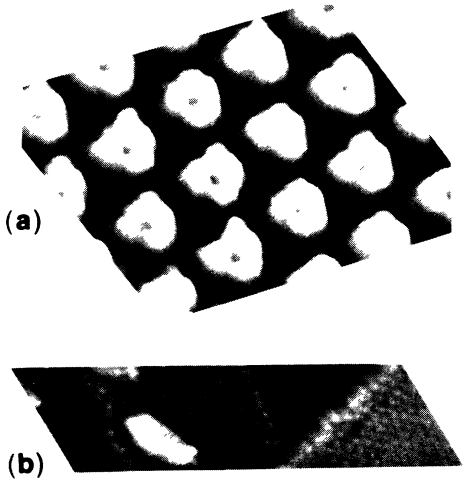

FIG. 4. (a) A three-dimensional view of the image in Fig. 3(b) from the right side emphasizes the ringlike appearance. (b) Three steps and the (3×3) superlattice on each (111) terrace are visible in this 300×90-Å^2 image. $V_t = -1.25$ V and $i_t = 4$ nA. Statistical differencing (Ref. 11) has been used to reduce the apparent height of the atomic steps and defects in order to render the (3×3) corrugation visible.

Any explanation for the image contrast for benzene and CO must take account of the adsorbate electronic states. Some of the filled CO and benzene orbitals have been observed for Rh(111) and assigned with use of photoemission.[5] Inverse photoemission on other metal surfaces typically shows an empty $2\pi^*$ state[12,13] at least a few electronvolts above E_F for CO. Empty benzene e_{2u} levels[14] are found 5 eV above E_F for Cu(111) or Ag(111), but data are not available for Rh(111). However, an extended Hückel-theory calculation[15] for benzene bonded to a threefold hollow site on a Rh(111) cluster shows that the combination of the highest filled benzene state (e_{1g}) with metal orbitals in a bonding configuration shifts these occupied states a few volts further below E_F, in agreement with photoemission data,[5] while the same states combined in an antibonding configuration result in the existence of an empty antibonding Rh-benzene state just above E_F. In the present case, the existence of empty states near E_F which are partially localized on the π lobes of the benzene can easily account for large STM corrugations. The difficulty in imaging of CO molecules probably results from the lack of CO-Rh states near E_F. In principle, it should be possible to image the CO $2\pi^*$ states with higher bias voltages. If the STM is operated at higher voltages and lower currents, however, the corrugation is reduced. Operation at high currents, where the corrugation is larger because of the reduced tip-sample spacing, leads to instabilities, such as those evident in Fig. 4(b).

Other contributions to the image contrast between benzene and CO can be considered. Adsorbate-induced modifications to the potentials seen by tunneling electrons, which may be associated with local work-function changes,[1] would change the decay lengths of electronic wave functions. These work-function changes are known[5] for adsorbate-saturated Rh(111) surfaces ($\Delta\phi = +0.7$ for CO and $\Delta\phi = -1.3$ for benzene) and are consistent with the appearance of a protrusion for ben-

zene. The CO, however, would be expected to appear as an array of holes in the image, contrary to observation. Other differences, such as the different spatial distribution of the CO $2\pi^*$ state as compared to the e_{1g} benzene orbitals, may also be important. Data on other systems are needed to distinguish between these alternatives.

One pleasing result of this work is that one can image certain chemisorbed molecules by examing mixed metal-adsorbate states near E_F, thereby avoiding the use of high bias voltages which often damage the surface and tip. Although we cannot give a simple rule for predicting the magnitude of the corrugation to be expected for a particular molecule on a given metal surface, it is likely that large molecules, which have many closely spaced electronic states split by strong molecule-surface interactions, will often lead to states near E_F and result in a useful STM footprint. While the origin of the image contrast is not clear, its existence and symmetry allow one to obtain many of the advantages of high-resolution real-space imaging, possibly including the determination of molecular orientation and binding sites. In the present case, our STM images show nearly perfect surface order punctuated by occasional domain boundaries and defects, details of registration at steps, and a preview of surface-diffusion phenomena. Our results further suggest that coadsorption techniques may be helpful in reducing surface diffusion and for moving E_F closer to molecular states. STM on carefully chosen metal-adsorbate surfaces appears extremely promising for observations of surface chemical processes, such as molecular diffusion, nucleation phenomena, and step- or defect-related reactivity.

We are pleased to thank G. A. Somarjai for his encouragement and the loan of the Rh(111) crystal. We also thank I. P. Batra, E. L. Garfunkel, and M. A. Van Hove for valuable discussions. One of us (H.O.) gratefully acknowledges financial support from IBM Japan.

[a]Permanent address: IBM Japan, Ltd., Yamato Laboratory, 1623-14 Shimotsuruma, Yamato-shi, Kanagawa-ken 242, Japan. Current address: Material and Chemical Sciences Division, Lawrence Berkeley Laboratory, and Department of Chemistry, University of California, Berkeley, CA 94720.

[1]G. Binnig and H. Rohrer, IBM J. Res. Dev. **30**, 355 (1986).

[2]R. J. Behm, W. Hosler, E. Ritter, and G. Binnig, Phys. Rev. Lett. **56**, 228 (1986); E. Ritter, R. J. Behm, G. Potsche, and J. Wintterlin, Surf. Sci. **181**, 403 (1987).

[3]J. K. Gimzewski, E. Stoll, and R. R. Schlittler, Surf. Sci. **181**, 267 (1987).

[4]C. M. Mate and G. A. Somorjai, Surf. Sci. **160**, 542 (1985), and references therein.

[5]E. Bertel, G. Rosina, and F. P. Netzer, Surf. Sci. **172**, L515 (1986).

[6]R. F. Lin, G. S. Blackmann, M. A. Van Hove, and G. A. Somorjai, Acta Crystallogr. Sect. B **43**, 368 (1987).

[7]S. Chiang, R. J. Wilson, Ch. Gerber, and V. M. Hallmark, J. Vac. Sci. Technol. A **6**, 386 (1988).

[8]M. A. Van Hove and R. J. Koestner, in *Determination of Surface Structure by LEED,* edited by P. M. Marcus and F. Jona (Plenum, New York, 1984), p.357.

[9]S. Chiang, R. J. Wilson, C. M. Mate, and H. Ohtani, to be published.

[10]V. M. Hallmark, S. Chiang, J. F. Rabolt, J. D. Swalen, and R. J. Wilson, Phys. Rev. Lett. **59**, 2879 (1987).

[11]R. J. Wilson and S. Chiang, Phys. Rev. Lett. **59**, 2329 (1987), and J. Vac. Sci. Technol. A **6**, 398 (1988).

[12]J. Rogozik, V. Dose, K. C. Prince, A. M. Bradshaw, P. S. Bagus, K. Herrman, and Ph. Avouris, Phys. Rev. B **32**, 4296 (1985).

[13]S. Ferrer, K. H. Frank, and B. Reihl, Surf. Sci. **162**, 264 (1985).

[14]K. H. Frank, R. Dudde, and E. E. Koch, Chem. Phys. Lett. **132**, 83 (1986).

[15]E. L. Garfunkel, C. Minot, A. Gavezzotti, and M. Simonetta, Surf. Sci. **167**, 177 (1986).

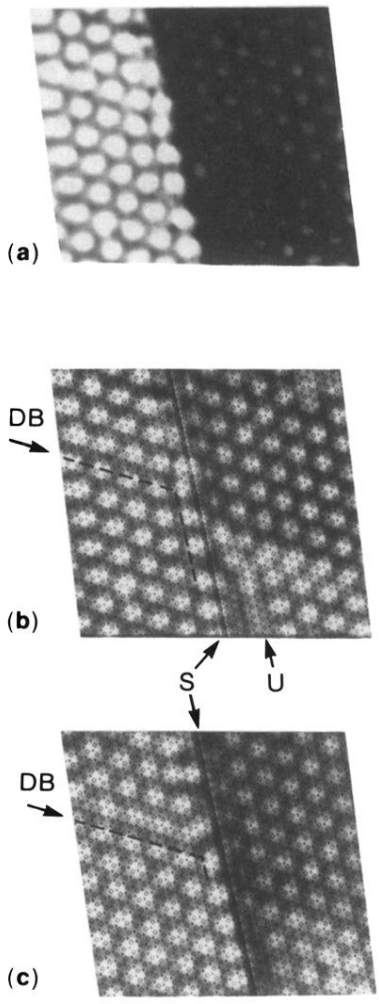

FIG. 2. Three images of the 3×3 superlattice extending across an atomic step. For each terrace, the first- and second-layer Rh atoms are represented by big and small lozenges, respectively. Images were recorded with tip bias $V_t = -1.25$ V and tunnel current $i_t = 4$ nA. (a),(b) Images derived from the same data, (c) image recorded about 10 min later.

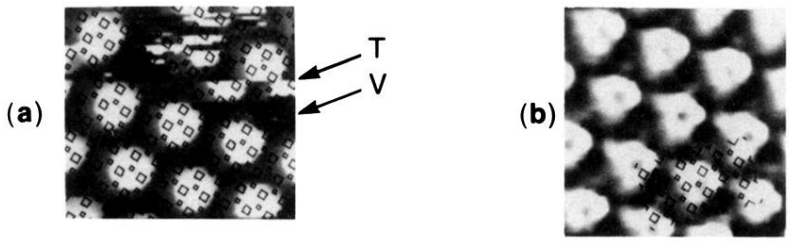

FIG. 3. (a) At high bias the benzene images become flat topped, nearly cylindrical, and 2 Å high, but the tip and surface appear unstable. (b) At lower bias, $|V_t| < 0.5$ V, a nominally threefold structure with a depression at the center is observed. According to the superimposed mesh based on the LEED model, the lobes appear to be localized between, rather than over, the underlying metal atoms.

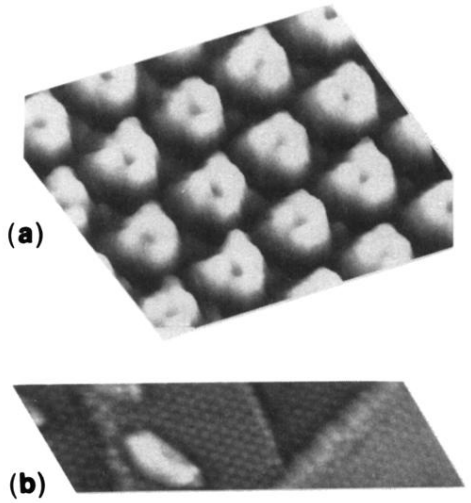

FIG. 4. (a) A three-dimensional view of the image in Fig. 3(b) from the right side emphasizes the ringlike appearance. (b) Three steps and the (3×3) superlattice on each (111) terrace are visible in this 300×90-Å^2 image. $V_t=-1.25$ V and $i_t=4$ nA. Statistical differencing (Ref. 11) has been used to reduce the apparent height of the atomic steps and defects in order to render the (3×3) corrugation visible.